Angular resolution improvement by using multi-radar and FBSS MUSIC DoA estimation algorithm

Paaso, Henna; Hirvonen, Mervi

Published in:
2019 IEEE Intelligent Vehicles Symposium, IV 2019

DOI:
10.1109/IVS.2019.8813780

Published: 01/06/2019

Document Version
Early version, also known as pre-print

Angular Resolution Improvement by Using Multi-Radar and FBSS MUSIC DoA Estimation Algorithm

Henna Paaso[1] and Mervi Hirvonen[2]

***Abstract*— In this paper, our goal is to improve angular resolution of 77 GHz radar with eight receiver channel by using a multi-radar system and high-resolution direction-of-arrival (DoA) estimation algorithm. The theoretical and experimental results show that angular resolution can be improved 42.6% with multi-radar system compared to a single radar system when two targets have exact the same distances from the radar. In this paper, we also show experimental studies for forward backward spatial smoothing (FBSS) multiple signal classification (MUSIC) DoA estimation algorithm. The algorithm is demonstrated in a real world indoor environment and the results of the estimated DoAs showed considerably good agreement with the predicted angles. By using this algorithm, angular resolution can be improved 40.8% compared to fast Fourier transform (FFT) beamforming (BF) algorithm.**

I. Introduction

A high-resolution capability is one of the most important requirement for radar of an autonomous driving system [1]. Radars work in all weather conditions (fog, rain, smoke, bright sunlight, darkness), but the resolution is poor compared to optical sensors. Target resolution is defined as the capability of distinguish two targets that are very close together in either range or angle. Range and angular resolutions depend on the physical parameters of the radar. The range resolution depends on the bandwidth of the transmitted signal and the angular resolution directly depends on the dimension of the antenna [2]. Thus, high-resolution capability is very difficult for the small-sized automotive radar [1].

One goal is to get cheap sensors, thus the number of antennas M and the number of snapshots K are limited [3]. However, to get reasonable results, the direction-of-arrival (DoA) estimator must be as good as possible. When targets are closely spaced, fast Fourier transform (FFT) beamforming (BF) technique cannot separate two targets. Thus, high-resolution DoA estimation algorithms are required, which can overcome the limitation of the antenna size.

In the frequency-modulated continuous-wave (FMCW) radar system, one major challenge is the low number of snapshots and significantly varying signal-to-noise ratio (SNR) [4]. DoA estimation algorithms using the low number of snapshots have been introduced by [1], [3], [5], [6], [7], [8], [9], [10]. In frequency domain, only one to three bins can be used for angle estimation [9]. In the FMCW radar case, received signals are often correlated. The degree of correlation is relative to the situation. It could be close the coherence, which can be considered as the worst situation for high-resolution DoA estimation algorithms [9]. However, using decorrelation algorithms, like as forward backward spatial smoothing (FBSS), increases the performance for correlated signals and for uncorrelated scenarios as smoothing virtually improves the number of snapshots [9].

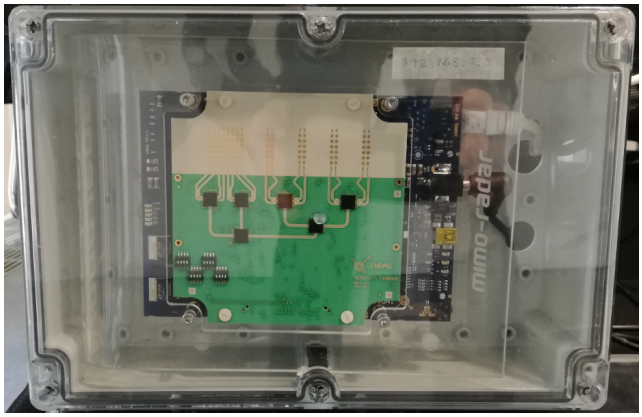

Fig. 1: INRAS 77 GHz radar.

In this paper, we introduce how multi-radar system and DoA estimation algorithm can improve angular resolution and reliability. In multi-radar system, data of two radars is combined for better angular resolution. Chapter II introduces the results of the theoretical and real-world measurements for multi-radar system. In Chapter III, studies of the DoA estimation algorithms for FMCW radar and experimental measurements are described. Finally, Chapter IV presents conclusions.

II. Multi-Radar System

A. 77 GHz Radar

In this paper, we have used 77 GHz multiple-input and multiple-output (MIMO) FMCW radar that is test/development kit by INRAS GmbH [11]. It is illustrated in Fig. 1. The main features of the radar include four transmitter (TX) channels, eight receiver (RX) channels (RRN7745) with differential IF outputs. In this paper, we use only single TX channel because the autonomous cars detect the moving targets in which case the usage of time domain MIMO is challenging [12]. The theoretical angular resolution directly depends on the dimension of the

*This work has been performed in the framework of the H2020-ECSEL-2015 Project DENSE and HISENS project by Academy of Finland.

[1]Henna Paaso and Mervi Hirvonen are with VTT Technical Research Centre of Finland, [1]90571 Oulu, [2]02044 Espoo, Finland {Henna.Paaso, Mervi.Hirvonen}@vtt.fi

Fig. 2: The maximum distance of the radars in the Martti robot car.

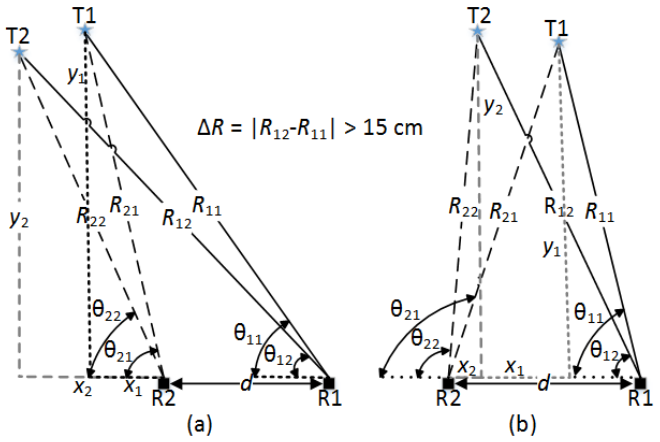

Fig. 3: Range resolution effects on the targets detection: (a) $\theta_{22} \leq 90°$ and $\theta_{21} \leq 90°$ and (b) θ_{22}>90° and θ_{21}>90°.

TABLE I: Summary of the simulation results for angular resolution 9.7°

Distance between radars (m)	Range of θ_{22} (°)	Spatial range (°)	Range of θ_{12} (°)
1.19	-36 <θ_{22}< 47	52	-45.6 <θ_{12}< 35.9
1.31	-42 <θ_{22}< 52	81	-51.4 <θ_{12}< 40.5
1.49	-48 <θ_{22}< 58	96	-57.3 <θ_{12}< 46.1
1.61	-51 <θ_{22}< 60	104	-60.2 <θ_{12}< 7.4

TABLE II: Summary of the simulation results for angular resolution 6.7°

Distance between radars (m)	Range of θ_{22} (°)	Spatial range (°)	Range of θ_{12} (°)
1.19	-	0	-
1.31	0 <θ_{22}< 23	23	-14.7 <θ_{12}< 7.8
1.49	-19 <θ_{22}< 42	61	-33.4 <θ_{12}< 26.5
1.61	-25 <θ_{22}< 48	73	-39.4 <θ_{12}< 32.2

antenna and it can be defined by $\theta_{\text{res}} \approx 59°\lambda/L$ where $L = (M-1)d$, where d is the distance between elements [2]. For INRAS radar, $d = \lambda/2$ where λ is wavelength. Thus, the angular resolution is 16.9°. Additionally, the range resolution ΔR is 15 cm for this radar which bandwidth B is 1 GHz ($\Delta R = c/2B$, c is the speed of light). More featured of the radar can be found from [11].

B. Theoretical Studies for Multi-Radar System

In this paper, we show how much a multi-radar system improves angular resolution in a theory. As we know, our used 77 GHz radars have 16.9° angular resolution. In the multi-radar system, data of two radars is combined. Fig. 2 illustrates how two radars could be placed in VTT's robot car, Martti. The maximum distance between two radars is 1.61 m (1.8 m - 0.19 m = 1.61 m), as illustrated in Fig. 2.

We know that the range resolution is 15 cm for the 77 GHz radar. By using this range resolution value, we can theoretically define how much two radars can improve the angular resolution, as illustrated in Fig. 3 where distances of the both targets (T1 and T2) from radar 2 (R2) are the same, $R_{22} = R_{21}$. Thus, if the difference between distances R_{11} and R_{12}, $\Delta R = |R_{12} - R_{11}|$, is bigger than 15 cm then the radar 1 (R1) can separate the targets.

The angular resolution can be defined by using basic geometry equations. Fig. 3(a) illustrates the locations of the targets, when $\theta_{22} \leq 90°$ and $\theta_{21} \leq 90°$. If $\theta_{22} \leq 90°$, then x_2, y_2, and θ_{12} can be defined as $x_2 = R_{22}\cos\theta_{22}, y_2 = R_{22}\sin\theta_{22}$, and $\theta_{12} = \tan^{-1}(\frac{y_2}{x_2+d})$. If $\theta_{21} \leq 90°$, x_1, y_1, and θ_{11} can be expressed as $x_1 = R_{21}\cos\theta_{21}, y_1 = R_{21}\sin\theta_{21}$, and $\theta_{11} = \tan^{-1}(\frac{y_1}{x_1+d})$. After $x_2, x_1, y_2, y_1, \theta_{12}$ and θ_{11} are defined, we can defined $R_{12} = \frac{x_2+d}{\cos\theta_{12}}$ and $R_{11} = \frac{x_1+d}{\cos\theta_{11}}$. Finally, ΔR can be calculated. If ΔR is more than 15 cm, R1 can separate these two targets.

Fig. 3(b) presents the positions of the targets, when θ_{22}>90° and θ_{21}>90°. If θ_{22}>90°, x_2, y_2, and θ_{12} can be defined as $x_2 = R_{22}\cos(180° - \theta_{22}), y_2 = R_{22}\sin(180° - \theta_{22})$, and $\theta_{12} = \tan^{-1}(\frac{y_2}{d-x_2})$. If θ_{21}>90°, then x_1, y_1, and θ_{11} can be calculated as $x_1 = R_{12}\cos(180° - \theta_{21}), y_1 = R_{12}\sin(180° - \theta_{21})$, and $\theta_{11} = \tan^{-1}(\frac{y_1}{d-x_1})$. After that, we can calculate $R_{12} = \frac{d-x_2}{\cos\theta_{12}}$, $R_{11} = \frac{d-x_1}{\cos\theta_{11}}$, and ΔR. The Matlab simulation model has been made by using above equations that we can see how the different locations of the targets and distance between two radars effect on the angular resolution.

Tables I-II and Fig. 4 present the summary of the results. The distance from targets to R2 is 5 m and distance between radars varies from 1.19 m to 1.61 m. From our results, we can see how the different locations of the targets and distance between two radars effect on the angular resolution. It can be seen that if the distance between radars are larger, the better angular resolutions can be achieved. If the distance between radars is 1.31 m, 9.7° angular resolution can be achieved in 81° spatial range, as shown in Fig 4(a) and Table I. Additionally, if angular resolution is decreased to 6.7°, then the spatial range is only 23°, as illustrated in Fig. 4(b) and Table II. In summary, the angular resolution can be improved 42.6% in 81° spatial range compared to a single

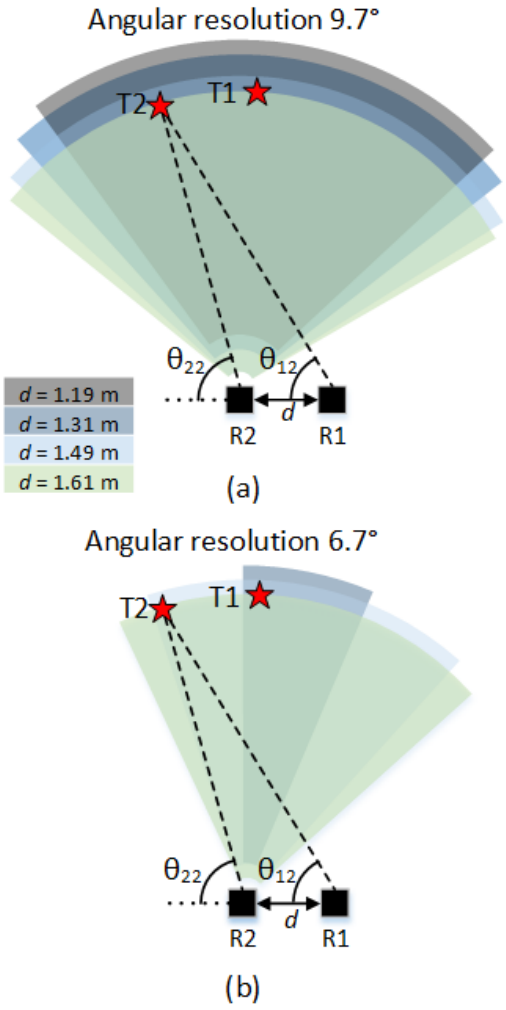

Fig. 4: Spatial range: Angular resolution is 9.7° and 6.7°.

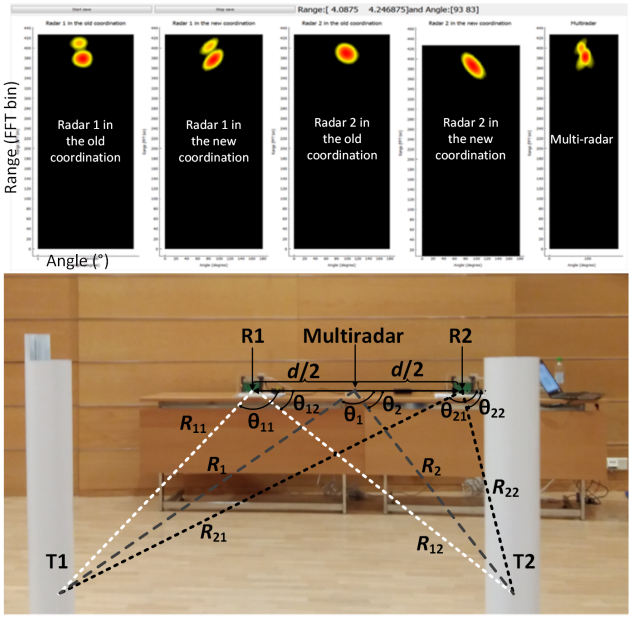

Fig. 5: The coordination change of the multi-radar system.

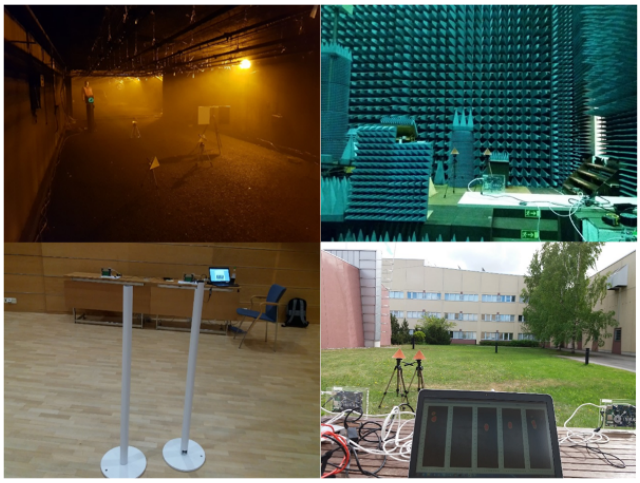

Fig. 6: Different kinds of measurement environments.

radar system when two targets have the exact same distances from the radar.

C. Combining the Data of Two Radars

In this section, we show how two radars (R1 and R2) FFT-maps can be combined to one FFT map, as illustrated an example measurement case in Fig. 5. This means that the coordinations of both radars have to transform into middle of the radars. This can be done by defining how much range and angle dimensions change when coordination of radars change to middle of the radars. First, the change of ranges is calculated: $\Delta r_{11} = R_{11} - R_1$, $\Delta r_{12} = R_{12} - R_2$, $\Delta r_{21} = R_{21} - R_1$, and $\Delta r_{22} = R_{22} - R_2$. Then, we know that one-step size of the range is 9.375 mm for our radars. We can calculate number the steps: $\frac{\Delta r_{ij}}{9.375\text{mm}}$, where i and j are 1 or 2. Number of the steps in angle case can be defined in the same way: $\Delta\theta_{11} = \theta_{11} - \theta_1$, $\Delta\theta_{12} = \theta_{12} - \theta_2$, $\Delta\theta_{21} = \theta_{21} - \theta_1$, and $\Delta\theta_{22} = \theta_{22} - \theta_2$.

On left side figure, the FFT map of the R1 is illustrated in the old coordination. In the second plot, the coordination of the R1 is transformed into the coordination of the middle of the radars. The third plot illustrates FFT map of the R2 in the old coordination. In the fourth plot, the coordination of the R2 is transformed into the coordination of the middle of the radars. The last plot illustrates the multi-radar, thus two radars FFT-maps are combined to one FFT map. From the figure, we can note that two radars see targets differently, thus we can improve the angular resolution by using FFT-maps of two closely separated radars, as we already noticed from the theoretical results in the last section IIB.

D. Experimental Studies for Multi-Radar System

Next, real-world measurements show that the same improvements for the angular resolution, as in theoretical simulations, can be also achieved. We have tested 77 GHz multi-radar system in different kinds of environments: Cerema in fog and rain environments, VTT's anechoic chamber room, lecture room, and outdoor environments, as

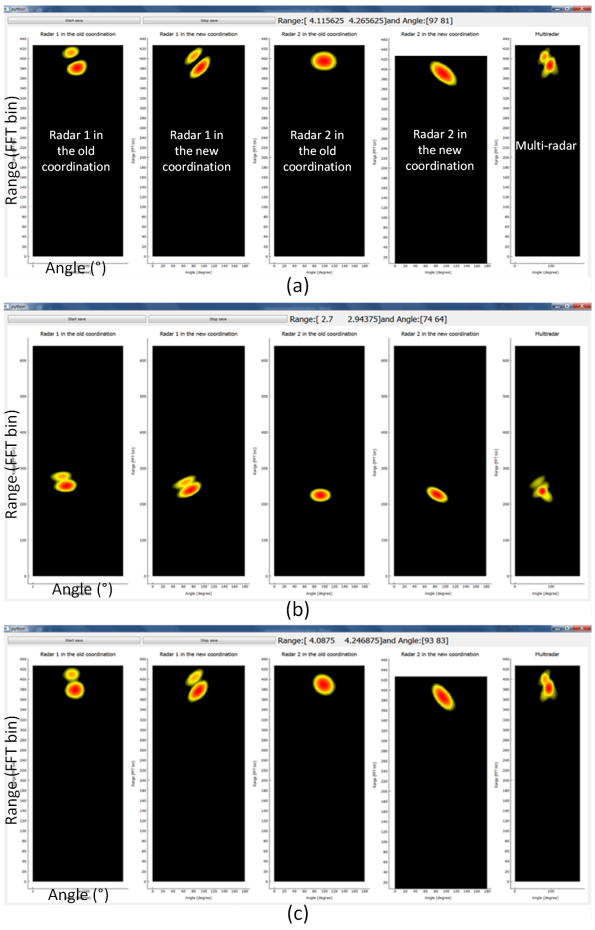

Fig. 7: Example measurement cases: (a) $\theta_{res} = 9.8°, R_{22} = R_{21} = 4$ m, d =1.29 m, $d_T = 68$ cm, (b) $\theta_{res} = 7.6°, R_{22} = R_{21} = 2.5$ m, d =1.29 m, $d_T = 33$ cm, and (c) $\theta_{res} = 6.7°, R_{22} = R_{21} = 4$ m, d =1.29 m, $d_T = 46.4$ cm.

illustrated in Fig. 6. Our fog and rain measurements showed that even high rain and fog weather conditions does not have any large effects on the detection performance of the radar.

Fig. 7 illustrates the example results of the measurements. The description of the figures is clarified in section IIC. Two targets are located at the same distance, $R_{21} = R_{22}$, from R2 in all measurement cases. The distance between radars is 1.29 m and the distance of targets from R2 varies from 2.5 to 4 m. From the figures, we can see that the R1 and R2 can see targets differently. The R1 can detect two targets, whereas the R2 cannot separate these two targets. In all these example cases, the angular resolution is about 6.7°- 9.8°, as seen in Fig. 7. Thus, results of these real-world measurements correspond to the theoretical results.

From theoretical and measurement studies, we should note that this angular resolution improvement could be achieved only if the both targets distances are exact the same for the one radar. Additionally, it is good to notice that if we could use radars, which have bigger antenna arrays and the angular resolution of the radar is better than 9.7° (or 6.7° in small spatial range), two radars will not improve the angular resolution, then they could improve only reliability.

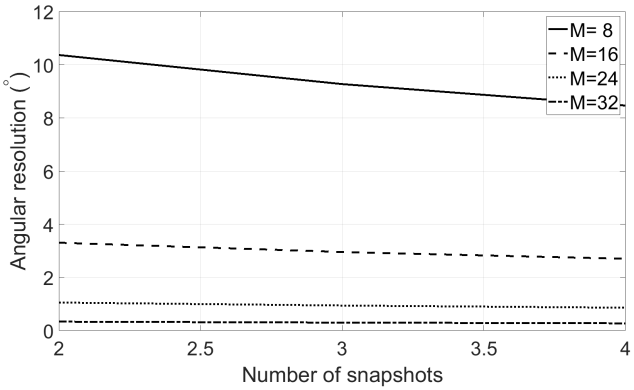

Fig. 8: Effect on number of snapshots and number of antenna elements on the angular resolution.

III. DoA Estimation for Radar

In this paper, BF spectrum is calculated using an FFT until now. However, the angular resolution (θ_{res}) directly depends on the aperture size. In our used 77 GHz radar, the angular resolution is 16.9°. Thus, the BF spectrum can be efficiently measured using an FFT if the angular resolution is greater than θ_{res}. However, two targets cannot be distinguished in the BF spectrum if the angular resolution is smaller than θ_{res}.

In paper [8], authors are evaluated the effect of small number of snapshots and SNR on the efficiency of MUSIC estimations. They present an expression that relates the broadside resolution $\theta_{\text{res}}^{\text{DoA}}$

$$\theta_{res}^{\text{DoA}} \cong 65 \exp(-M/7)(K+2)^{-0.5} \quad M, K \in I, 4 \leq M \leq 12, 2 \leq K \leq 10. \tag{1}$$

In Fig. 8, the broadside angular resolution versus number of snapshots for different number of elements is presented. From this figure, we can see that 10.4° angular resolution is achieve when $K = 2$ and $M = 8$. Additionally, we can see that 0.4° angular resolution can be achieved with large antenna arrays, when $K = 2$ and M = 32.

A. FBSS MUSIC

In our radar test system, ranges of the targets are estimated by using first FFT-transform and DoA estimation is made after FFT for each range FFT bin. Thus, the DoA estimation algorithm can only use a single snapshot for these estimated targets. For this reason, usually only one or two goals need to be estimated with a single snapshot [3]. In [1], [7], [9], authors has used FBSS MUSIC [13] DoA estimation algorithm for FMCW radar. In [7], they uses multi-chirp signal to improve angular resolution. In our radar system, we have used the same algorithm but we used only two snapshots to estimate DoAs and the performance of the algorithm is studied using real measurements.

We assume that L coherent signals receives $x(t)$ to the M uniform linear array (ULA). In our measurements, $L = 2$.

The basic idea of the spatial smoothing method is to divide the ULA into overlapping forward and backward subarrays of size P. In our case, $M = 8, P = 6$, and $Q = 3$, Q is number of the subarrays. We can define the received signals at the qth forward subarray [1]

$$X_q^{\mathrm{f}}(t) = [x_l(t)\ x_{l+1}(t)\ \cdots\ x_{l+P-1}(t)]^{\mathrm{T}} \tag{2}$$

and the backward subarray

$$X_q^{\mathrm{b}}(t) = [x_{M-l+1}^*(t)\ x_{M-l}^*(t)\ x_{M-l-1}^*(t)\ \cdots\ x_{Q-l+1}^*(t)]^{\mathrm{T}}. \tag{3}$$

The average covariance matrix of the forward subarrays $\mathbf{R}^{\mathrm{f}}$ and the backward subarrays $\mathbf{R}^{\mathrm{b}}$ can be presented as [1]

$$\mathbf{R}_{\mathrm{f}} = \frac{1}{Q}\sum_{q=1}^{Q} E[X_q^{\mathrm{f}}(t) X_q^{\mathrm{f}^H}(t)] \tag{4}$$

$$\mathbf{R}_{\mathrm{b}} = \frac{1}{Q}\sum_{q=1}^{Q} E[X_q^{\mathrm{b}}(t) X_q^{\mathrm{b}^H}(t)]. \tag{5}$$

The forward and backward spatial smoothed covariance matrix can be expressed as [1]

$$\mathbf{R}_{\mathrm{fb}} = \frac{\mathbf{R}_{\mathrm{r}} + \mathbf{R}_{\mathrm{b}}}{2}. \tag{6}$$

Once the FBSS covariance matrix is created, we can use an eigenvalue decomposition to compute the noise subspace matrix $\mathbf{E}_{\mathrm{N}}$. Finally, the FBSS MUSIC pseudospectrum can be written as

$$P_{\mathrm{FBSS}}(\theta) = \frac{1}{\mathbf{a}^H(\theta)\mathbf{E}_{\mathrm{N}}\mathbf{E}_{\mathrm{N}}^H\mathbf{a}(\theta)} \tag{7}$$

where $\mathbf{a}(\theta)$ is the steering vector, which can be expressed as $\mathbf{a}(\theta) = [1, e^{j2\pi\frac{d}{\lambda}\sin(\theta)}, \cdots e^{j2\pi(M-1)\frac{d}{\lambda}\sin(\theta)}]^{\mathrm{T}}$. The maximum values of pseudospectrum $P_{\mathrm{FBSS}}(\theta)$ will give the estimated DoAs of the received signals, $\hat{\varphi}$.

B. Experimental Results for FBSS MUSIC Algorithm

The performance of the FBSS MUSIC DoA estimation algorithm is evaluated using experimental measurements carried out in a real world indoor environment. The experiments are done in the premises of VTT Technical Research Centre of Finland, Oulu. The indoor setup is a large lecture room, as shown in Fig. 9. The figure depicts also the arrangement of radar and targets. We used one radar and nine target locations. Each of the targets were metallic poles and the radar was 77 GHz radar that is test/development kit by INRAS GmbH. We measured the targets and radar locations carefully with a laser measure. Finally, the basic geometry was used for the calculation of real DoAs, φ. The measurements were performed in such a way that only two target pair was on the floor at a time. The most difficult case for radars are separate targets, when they are at the same distance from the radar. Thus, we made measurements for seven scenarios where both targets are located at the same distances from the radar, $R_{12} = R_{11} = 3.5$ m, as described in Table III. In all measurement cases, the angular resolution

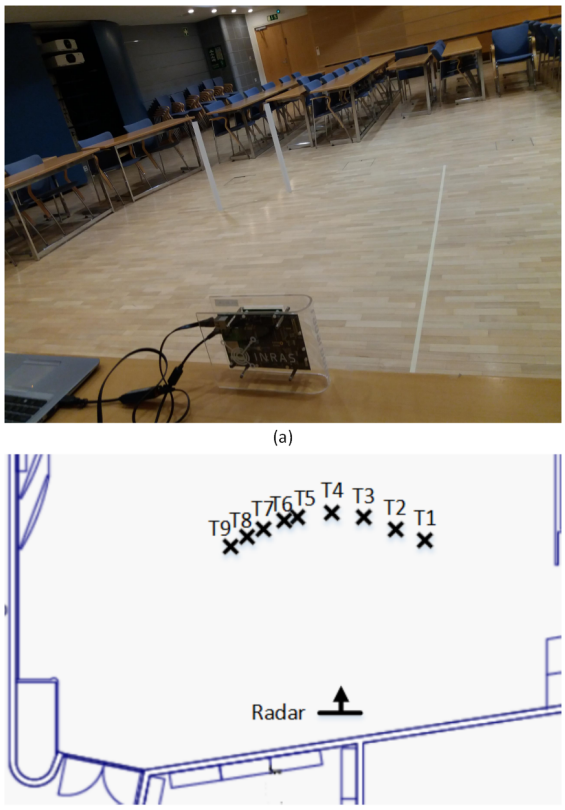

(a)

(b)

Fig. 9: Measurement environment in the lecture room (a) and layout of the measurement area (b).

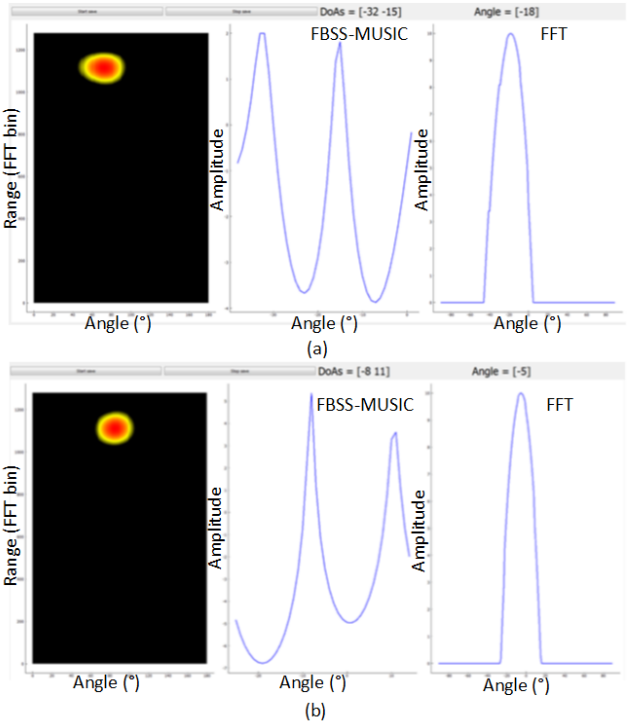

Fig. 10: DoA estimation results with FBSS MUSIC and FFT methods for the scenario T5-T7 (a) and T3-T4 (b).

TABLE III: Summary of the DoA estimation results for FBSS MUSIC algorithm

Scenarios	φ (°)		**FFT** $\hat{\varphi}_{FFT}$ (°)	**MUSIC-FBSS** $\hat{\varphi}$ (°)		**MUSIC-FBSS** ϵ (°)	
T*-T**	T*	T**		T*	T**	T*	T**
T1-T2	27	17	27	33	14	6	3
T2-T3	17	7	9	23	0	6	7
T3-T4	7	-3	-5	11	-8	5	4
T4-T5	-3	-13	-5	2	-15	5	2
T6-T8	-28	-17	-20	-26	-10	2	7
T5-T7	-13	-23	-18	-15	-32	2	9
T7-T9	-23	-34	-34	-20	-40	3	6
RMSE of ϵ (°)						4.5	5.7

between two targets was 10°. We used two snapshots to estimate DoAs.

The summary of the measurements for the FBSS MUSIC and FFT BF algorithms is presented in Table III, which includes also the individual DoA estimation error, ϵ. These results show that 10° angular resolution can be also achieved in real-world measurements. Thus, the results correspond to the theoretical results. The total root mean square error (RMSE) is calculated over all measurement scenarios. It is 5.2° for the FBSS MUSIC algorithm. Thus, the estimated DoAs match fairly accurately in all scenarios. Fig. 10 presents the DoA estimation results for the scenarios T5-T7 and T3-T4 as a function of the DoA for the FBSS MUSIC and FFT BF algorithms. On the left side figure, the plot illustrates the FFT map of the radar. Middle of the plot show the FBSS MUSIC pseudo-spectrum and right side figure illustrates the FFT BF spectrum for the estimated range FFT bin.

We also have tested the FBSS MUSIC algorithm by using only a single snapshot. However, the results show that the algorithm does not give a steady result; the places of the peaks of the FBSS MUSIC spectrum vary very fast even when the environment is unchanged. We noticed the same phenomenon when the angular resolution is less than about 10°. However, we can conclude that we improved angular resolution 40.8% by using the FBSS MUSIC algorithm.

IV. Conclusions

In this paper, we demonstrated how angular resolution of 77 GHz radar with eight receiver channel can be improved. We studied two different methods: 1) Using multi-radar system and 2) FBSS MUSIC DoA estimation algorithm. Our results shown that the angular resolution can be improved using these both methods.

The theoretical and experimental results shown that the angular resolution can be improved 42.6% with two radars when two targets have exact the same distances from the radar. The result also introduced that the distance between radars has big effect of the angular resolution value. If the distance is longer, then angular resolution is smaller for larger spatial area. Additionally, we noticed also following: If we could use radars, which have bigger antenna arrays and the angular resolution of the radar is better than 9.7°, two radars will not improve the angular resolution, they could only improve reliability.

We also studied, how much high-resolution DoA estimation algorithms can improve the angular resolution. We have selected FBSS MUSIC algorithm because it can estimate the DoA even the received signal are correlated. The theoretical simulations and the results of real-world measurements showed that we can achieve 10° angular resolution with eight receiver channel radar if two snapshots are used. Thus, the angular resolution was improved 40.8% by using the FBSS MUSIC algorithm compared to the FFT BF algorithm.

Acknowledgment

We would like to express our great appreciation to the whole DENSE project (Grant Agreement number: 692449) consortium for valuable discussions on the designing of the weather robust radar for automotive use. The project has been co-funded by ECSEL Joint Undertaking and national funding agencies like Business Finland and the Federal Ministry of Education and Research in Germany. The work was also partly funded by the HISENS-project (310879) by Academy of Finland.

References

[1] C.-H. Cha, D. Yeom, and E. Kim, "Implementation of high resolution angle estimator for an unmanned ground vehicle," *Journal of Electromagnetic Engineering and Science*, vol. 15, no 1, pp. 37−43, Jan. 2015.

[2] M. Schneider, "Automotive radar status and trends," in *Proc. of the German Microwave Conference (GeMIC 2005)*, 2005, pp. 144−147.

[3] P. Häcker and B. Yang, "Single snapshot DoA estimation," *Advances in Radio Science*, vol.8, pp. 251−256, 2010.

[4] P. Wenig, M. Schoor, O. Gunther, B. Yang, and R. Weigel "System Design of a 77 GHz Automotive Radar Sensor with Superresolution DOA Estimation," *System and Electronics International Symposium on Signals, Systems and Electronics*, 2007. pp. 537−540.

[5] Q. S. Ren and A. J. Willis, "Extending MUSIC to single snapshot and on-line direction finding applications," in *Proc. of the IET International Conference on Radar*, pp. 783−787, October 1997.

[6] Chinese patent, "Single-snapshot data-based coherent signal DOA (direction of arrival) estimating method," priority date: 16.03.2015, CN104698433A.

[7] J. Choi, J. Park, and D. Yeom, "High angular resolution estimation methods for vehicle FMCW radar," in *Proc. of 2011 IEEE CIE International Conference on Radar*, 2011, pp. 1868−1871.

[8] G. A. Ioannopoulos, D. E. Anagnostou, M. T. Chryssomallis, "Evaluating the effect of small number of snapshots and signal-to-noise-ratio on the efficiency of MUSIC estimations," *IET Microw. Antennas Propag.*, 2017, vol. 11, no 5, pp. 755−762.

[9] M. Schoor and B. Yang B, "High-Resolution Angle Estimation for an Automotive FMCW Radar Sensor," *Semantic Scholar*, 2011.

[10] C.-J. Huang, C.-V. Dai, T.-Y. Tsai, W.-H. Chung, and T.-S. Lee, "A closed-form phase-comparison ML DoA estimator for automotive radar with one single snapshot," *IEICE Electronics Express*, vol. 10, no. 7, pp. 1−7, 2013.

[11] MIMO-77-TX4RX8 Frontend, User manual. [Online]. Available: $http : //www.inras.at/uploads/media/MIMO - 77 - TX4RX8_01.pdf$. [Accessed: 31- Jan- 2019].

[12] C. M. Schmid, R. Feger, C. Pfeffer, and A. Stelzer "Motion Compensation and Efficient Array Design for TDMA FMCW MIMO Radar Systems," in *Proc. 6th European Conference on Antennas and Propagation (EUCAP)*, 2011, pp. 1746−1750.

[13] T. J. Shan, M. Wax, and T. Kailath, "On spatial smoothing for direction of arrival of coherent sources," *IEEE Transactions on Acoustics, Speech and Signal Processing*, vol. 33, pp. 806−811, Aug. 1985.